PHYSICAL REVIEW B VOLUME 45, NUMBER 20 15 MAY 1992-II

Structural and electronic properties of K/Si(100)2×1

E. G. Michel,* P. Pervan,† G. R. Castro, R. Miranda,* and K. Wandelt
Institut für Physikalische und Theoretische Chemie, Universität Bonn, Wegelerstrasse, 12 D-5300 Bonn 1, Federal Republic of Germany
(Received 28 March 1991; revised manuscript received 1 July 1991)

The interface K/Si(100)2×1 has been investigated by using a variety of surface techniques sensitive to both structural and electronic properties. The adsorption site of potassium was determined by using Xe titration and Xe photoelectron spectroscopy. Potassium atoms are preferentially adsorbed between the rows of dimers of the 2×1 reconstruction (cave-valley sites). Controversy exists about the degree of ionicity of the K—Si bond, and the way the surface is metallized after K adsorption. Using work-function change, thermal desorption, and ultraviolet photoemission measurements, we determined that the potassium overlayer has metallic character above 0.5-monolayer (ML) coverage. We have studied by means of photoemission of adsorbed xenon the way the surface potential is affected by K adsorption. The charge transfer from K to Si gives rise to a reduction of the local work function at sites close to K atoms. In addition, a long-range reduction affects the whole surface from coverages of 0.2 ML on.

I. INTRODUCTION

Alkali metals have been extensively studied for a relatively long time, mainly because of their important role as additives in many catalyzed reactions, such as the synthesis of ammonia or the Fischer-Tropsch catalysis.[1] Due to the technological importance of alkali-metal–semiconductor interfaces, these systems have deserved widespread attention in the past few years.[2] Topics such as the activation of semiconducting surfaces to negative electron affinity (used in image intensifiers and infrared detectors),[3,4] spin-polarized electron guns, or the alkali-metal-promoted oxidation of semiconductors[5,6] shall be fully understood only once the microscopic properties of the alkali-metal–semiconductor interfaces are explained. Note only have the technological implications of these interfaces contributed to the general interest in these systems, but also the fascinating fundamental problems which appear during the formation of the interface. Alkali-metal–semiconductor interfaces constitute a well-defined model system where ideas about Schottky-barrier formation, charge transfer, and metallization can be tested in view of their application to more complex metal-semiconductor systems.[7] These interfaces are considered to be abrupt and nonreactive,[3,8] thus facilitating much more the task of studying the parameters involved in the formation of the interface, as compared to the case of transition metals, where reaction or interdiffusion frequently take place.[7] The systems Cs/Si(100)2×1 and in particular K/Si(100)2×1 have received great attention in the past few years, from both theoretical and experimental workers, in part because the Si(100)2×1 surface has been considered to be the simplest reconstruction of the high-symmetry faces of silicon.[9] As a consequence of these efforts many of their relevant properties have been measured and calculated. However, the systems are still a matter of controversy, and different and contradictory models have been put forward to explain the relevant experimental facts.[10–12] In view of the extensive literature published on these interfaces,[2,8,10–42] we refer the reader to Refs. 2 and 41 for an updated review, and will consider in the following only the information relevant to the experimental magnitudes measured in this paper.

The controversy about the fundamental properties of K/Si(100)2×1 involves in particular the K—Si bond length;[10–12,16] the metallic or semiconducting character of the interface and the nature of the metallization process;[8,14,15] and the adsorption site of the alkali-metal atoms.[3,10–12,17] Obviously, all three points are deeply interconnected and a full understanding of these interfaces will be achieved only when all three are clarified. We will consider in the following the last two properties in more detail. Before proceeding, it is convenient to clarify the concept of monolayer (ML). We define in this paper 1-ML coverage ($\Theta=1$) as a density of atoms equal to the atomic density of the Si(100) surface, i.e., 6.78×10^{14} atoms/cm^2. This is a suitable definition because the values of the coverages can be directly related to the number of K atoms present.

Concerning the metallization process and the nature of the K-Si bond, Tochihara[8] reported for K/Si(100)2×1 a saturation coverage of 0.5 ML at room temperature (RT) and a decrease of the work function of 2.1 eV without passing through a minimum. Aruga, Tochihara, and Murata performed angle-resolved electron energy loss spectroscopy[18] (EELS) and determined the dispersion of two loss peaks. These authors interpreted the bonding of K to the surface according to Levine's model for Cs/Si(100)2×1 (Ref. 3) (adsorption on the pedestal sites and formation of one-dimensional chains, see Fig. 1). On the basis of detailed calculations,[19,20] the observed loss peaks were attributed to the one-dimensional plasmons associated with the metallic K chains on the surface. Oellig and Miranda[21] observed for the first time that the

 ©1992 The American Physical Society

K-induced work-function change does, in fact, pass through a minimum before reaching the bulk value. The maximum decrease of the work function was 3.0 eV, a value much larger than the one reported by Tochihara.[8] The results of Ortega *et al.*[22] showed that Cs/Si(100)2×1 behaves in a similar way. Enta *et al.*[14,23] determined the band structure of K/Si(100)2×1 at saturation coverage. The surface at this coverage was semiconducting, and relatively unaffected by the K adsorption. The band structure for a one-domain Si(100)2×1 substrate was determined by Enta *et al.*[24] as well. Castro *et al.*[15] favored metallization over 0.5 ML (see also Sec. IV). Finally, metastable deexcitation spectroscopy (MDS) experiments by Nishigaki *et al.*[25] clearly indicated that the charge transfer from K to Si is small, even at very low coverages.

The adsorption site of the K atoms has remained up to now a controversial issue. Since the pioneering work of Levine,[3] where the pedestal site was proposed for Cs/Si(100), a larger number of authors have assumed this model, further favored by subsequent low-energy electron diffraction (LEED) studies.[31] Very recently XPD (x-ray photoemission diffraction) (Refs. 32 and 33) and AED (Auger electron diffraction) (Ref. 34) studies have been performed. XPD results indicate that at the RT equilibrium coverage the adatoms are sitting on both pedestal and valley sites. AED results point to the fact that the adsorption position of K is not the pedestal one, as previously assumed, but rather a mixture of pedestal and cave positions, depending strongly on the annealing temperature. Further information on the adsorption site can be extracted from the Xe thermal desorption data by Pervan *et al.* (Ref. 35, see also Sec. IV E). STM (scanning tunneling microscope) work on these interfaces has provided rather contradictory results. Badt *et al.*[36] observed a disordered adlayer; Hasegawa *et al.*[37] observed adsorption of Li and K at the on-top site[38] for low coverages followed by ordering in lines perpendicular to the dimer rows. Binder *et al.*[39] observed adsorption on the cave site. Finally, x-ray standing wave results by Eteläniemi, Michel, and Materlik[40] for Rb/Si(100)2×1 indicated adsorption on pedestal and valley sites for coverages close to 1 ML and promotion of the cave site after annealing. Theoretical studies generally supported Levine's model.[10] More recent calculations have favored, however, the cave site: Batra[17] concluded for Na/Si(100)2×1 that the pedestal and cave sites are equally favored. Ling, Freeman, and Delley[11] obtained total energies in the order of increasing stability for the bridge, pedestal, valley, and cave sites (see Fig. 1), $E(\text{bridge}) \simeq E(\text{pedestal}) \leq E(\text{valley}) \leq E(\text{cave})$, with bond lengths of 3.1, 3.2, 3.5, and 3.2 Å, close to the experimental value. Ramírez[12] obtained the same filling order for the four sites. Finally, Batra calculated the energetics of Na/Si(100)2×1 at different coverages.[41]

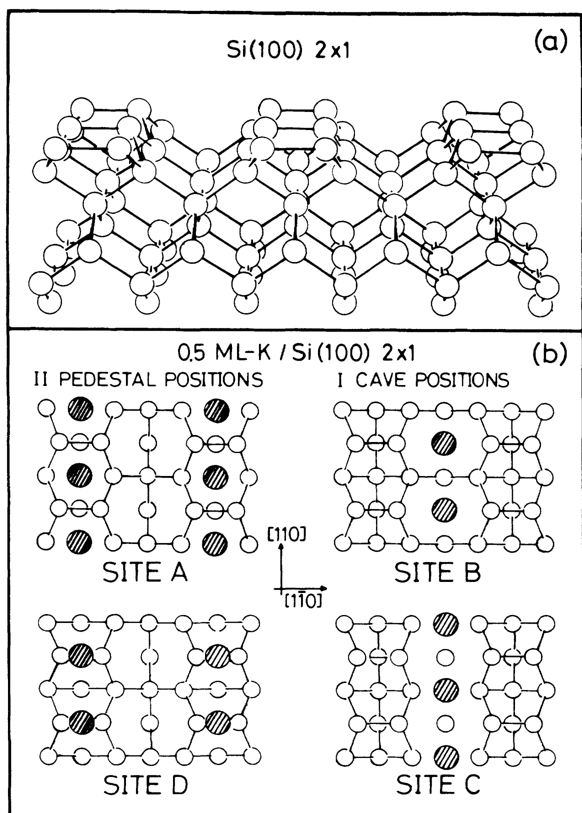

FIG. 1. Adsorption sites on Si(100)2×1. (a) Perspective view of the 2×1 reconstructed surface of Si(100). (b) Top view of the Si(100)2×1 surface covered with 0.5 ML of K. White circles: silicon atoms; dashed circles: potassium atoms. The different adsorption sites are shown: *A* (pedestal), *B* (cave), *C* (valley), and *D* (bridge). Sites *A* and *D* are generically labeled with number II as "pedestal positions," while sites *B* and *C* are labeled with number I as "cave positions."

The purpose of our work has been to shed some light on this debated system, where so much controversy exists, both from experimental and theoretical points of view. Our approach has consisted of carefully determining some of the properties of the system in order to clarify the debated issues, in particular the onset of metallization and the K adsorption site. As these properties are strongly dependent on the actual coverage, a careful coverage calibration was performed and cross-checked with different techniques. In this paper we will give a full account of our results, which have been partially presented elsewhere.[15,35,42] The paper is organized as follows: in Sec. II the experimental details are described; in Sec. III we will present our results for the clean Si(100)2×1 surface, relevant to the interpretation of the K/Si(100)2×1 ones; in Sec. IV the results for the K/Si(100)2×1 interface are presented; finally in Sec. V we will comment on the properties of this interface.

II. EXPERIMENT

The experiments were performed in an ultrahigh vacuum (UHV) chamber equipped with the standard analytical techniques LEED, AES (Auger electron spectroscopy) performed with a CMA (cylindrical mirror analyzer), TDS (thermal desorption spectroscopy), and UPS (ultraviolet photoemission spectroscopy, photon energy $h\nu=21.2$ eV). The Si(100) sample (n-type, 30–50 Ω cm,

$1\times10\times10$ mm^3) was cut from a commercial wafer. It was clamped onto a tantalum plate, which was fixed to the sample holder. The sample temperature could be controlled between 40 and 1300 K by means of a closed-loop He refrigerator, connected to the sample by a flexible copper braid, and resistive heating of the tantalum plate. The temperature was measured by a Cr-NiCr thermocouple spot welded to the back of the tantalum plate, in good thermal contract with the sample but far away to prevent any contamination. The temperature axis was properly calibrated by means of the heats of sublimation of a thick potassium film and of a thick Xe crystal, grown at low temperature, and desorbing from the Si(100)2×1 surface. The sample was cleaned by cycles of Ar^+ sputtering (2 keV, 5 μA), annealing at 1200 K during a few minutes, and slow cooling at a rate of 1 K/s. The surface thus prepared always displayed a sharp 2×1 LEED pattern. The ratio of the AES peak heights C_{270} and Si_{92} was less than $\frac{1}{2000}$, and no other impurities (in particular O, Ni, and Cu) could be detected by means of AES. The base pressure was 8×10^{-11} Torr. Potassium was evaporated by resistively heating a commercial dispenser (SAES-Getters, Italy), which was carefully degassed. During the K deposition the pressure never rose over 2×10^{-10} Torr.

Band-bending measurement

We briefly review in this section the employment of the saturation of the surface photovoltage (SPV) at low temperatures, as a tool to determine the overlayer metallization, and to measure the Schottky-barrier height versus adsorbate coverage.

The work function ϕ of a semiconductor can be represented as a sum of several contributions:[43] the potential energy difference due to the surface dipole layer (V_{SD}), which is chosen to be equal to the affinity energy (χ), the band bending (V_{BB}), and the chemical potential (μ) (see Fig. 2),

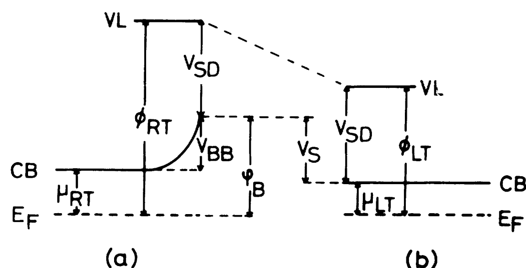

FIG. 2. Saturation of the surface photovoltage for K/Si(100)2×1. Part (a) (left) depicts the situation at room temperature (the bands are fully bent). Part (b) displays the bands at low temperature (55 K), while the surface is illuminated by ultraviolet light and the surface photovoltage is saturated. CB: conduction band; E_F: Fermi level; VL: vacuum level; V_{BB}: band bending; V_{SD}: dipole part of the work function; φ_B: Schottky barrier; ϕ_{RT} (ϕ_{LT}): work function at room temperature (low temperature); μ_{RT} (μ_{LT}): chemical potential at room temperature (low temperature).

$$\phi=V_{SD}+V_{BB}+\mu \ . \tag{1}$$

Usually $V_{BB}+\mu$ is called the Schottky barrier (φ_B). Illuminating the surface by very intense light makes it possible to depopulate (populate) the surface states, and accordingly decrease (increase) the Schottky barrier.[44] In the case of an n-type semiconductor, light-induced depopulation of the surface states will flatten the bands. This decrease of the band bending is observed as a decrease of the work function. The value for which the work function has been changed during exposure to the light is equal to the band bending and it is known in the literature as surface photovoltage. Demuth *et al.*[45] demonstrated that at temperatures around 50 K the electron-hole recombination is frozen for a silicon sample in such a way that it is possible to produce flatband conditions, even when the intensity of the light is about 10^{12} photons/cm^2 s. When an n-type silicon surface maintained at low temperature is illuminated by ultraviolet light of the He I line, the holes produced during the photoemission process accumulate at the surface region, and flatband conditions are achieved in a self-compensating process. For a detailed analysis of the values of the recombination speeds see Ref. 44. The effect is observed as a rigid shift to higher (for an n-type sample) or lower (for a p-type sample) binding energies of the UPS spectrum. It should be remembered that only a part of the shift is due to the saturation of the surface photovoltage. Another contribution is due to the temperature dependence of the chemical potential μ, which is smaller at low temperatures.[46,47] We shall use the abbreviations μ_{RT} and μ_{LT} for the values at RT and 50 K, respectively. For our sample doping $\mu_{RT}=0.3$ eV and $\mu_{LT}=0.1$ eV.[46,47] It can be directly deduced that the amount of the shift when decreasing the temperature from RT to 50 K (V_S) is

$$V_S=V_{BB}+\mu_{RT}-\mu_{LT} \tag{2}$$

because at low temperature, when the bands are flat, the work function is given by

$$\phi_{LT}=V_{SD}+\mu_{LT} \tag{3}$$

whereas at elevated temperatures, when the bands are fully bent, the work function is equal to

$$\phi_{RT}=V_{SD}+\mu_{RT}+V_{BB} \ . \tag{4}$$

Therefore one can determine the Schottky-barrier height by measuring the shift V_S.[45]

It is known also that the surface photovoltage can be saturated even if a certain amount of metal is present at the surface.[48] Considering Eqs. (3) and (4), at low temperatures a work-function change due to potassium adsorption represents the change of the surface dipole only (the chemical potential μ is a bulk parameter and is not affected by deposition of particles on the surface of the crystal),

$$\Delta\phi_{LT}=\Delta V_{SD} \ . \tag{5}$$

On the other hand, when the work function is measured at temperatures at which the band bending is fully developed,

$$\Delta\phi_{RT} = \Delta V_{SD} + \Delta V_{BB} . \quad (6)$$

Therefore the difference between the two curves ($\Delta\Phi$) corresponds to the pure band bending,

$$\Delta\Phi = \Delta\phi_{RT} - \Delta\phi_{LT} = \Delta V_{BB} . \quad (7)$$

There is, however, a critical amount of metal for which it is no longer possible to produce flatbands, since the adsorbed metal causes a drastic increase of the recombination speed of the charges accumulated at the surface, a process which accompanies the metallization of the overlayer. The actual amount of metal necessary to prevent the saturation of SPV can change very much in each case. It depends both on the properties of the metal and the semiconducting substrate, and on the type of growth of the metal (e.g., layer by layer, cluster formation, etc.).

III. THE Si(100)2×1 SURFACE: RESULTS AND DISCUSSION

The dimers of the Si(100)2×1 surface can be either symmetric (both atoms at the same height) or buckled (one atom is at a higher level than the other one). STM results have shown that well-prepared surfaces are formed by dimers which appear symmetric within the STM accuracy.[49] A certain amount of buckled dimers stabilized by defects is always present at the surface, although it can range from 3% to 30%, depending on the preparation conditions. Concerning the electronic structure, photoemission data have shown that the surface is semiconducting, with a filled surface state at about 0.7 eV below the Fermi level,[50,51] and an unoccupied state at about 0.3 eV above it.[52]

A. Valence-band spectra

Figure 3 shows the valence-band spectrum of the Si(100)2×1 surface taken both at 273 and at 55 K. The region closer to the Fermi level is displayed in more detail in Fig. 4 (bottom spectrum). The shoulder around 0.8 eV below the Fermi level (at 273 K) corresponds to the surface state, while the small emission at the Fermi energy (see Fig. 4, bottom spectrum) is attributed to the presence of defect states at the surface.[53] Note that the electrons detected by our spectrometer are strongly angle integrated, which enhances the intensity of this emission.[53] The photovoltaic shift of the valence-band spectrum at 55 K compared to the RT position (Fig. 3) is 0.6 eV. According to Eq. (2), the band bending V_{BB} is thus 0.4 eV, in close agreement with the measurements by Mönch, Koke, and Krueger.[54]

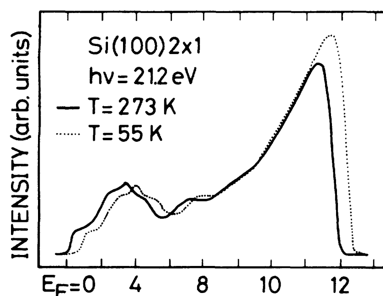

FIG. 3. Angle-integrated ultraviolet photoemission spectra for Si(100)2×1 taken at 273 (continuous line) and at 55 K (dotted line). The shift to higher binding energies observed at low temperature is due to the saturation of the surface photovoltage.

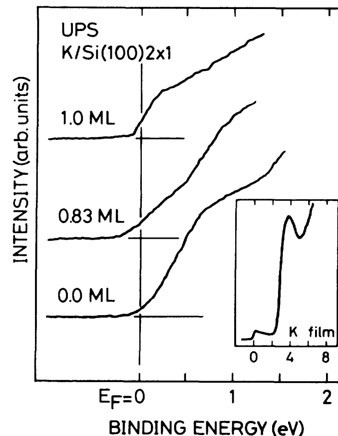

FIG. 4. Angle-integrated ultraviolet photoemission spectra for K/Si(100)2×1 at different coverages, taken at 273 K. Note the onset of the emission at the Fermi energy for at least 0.83 ML. Inset: a typical spectrum for a thick (~20 ML) K film.

B. Xenon adsorption on Si(100)2×1

1. Xenon thermal desorption spectroscopy

Figure 5 displays the Xe-TDS results for the Si(100)2×1 surface. The adsorption temperature and the Xe doses were carefully calibrated to avoid the growth of a second Xe layer. To this end, we selected an adsorption temperature higher than the desorption temperature of the second layer. On the other hand, the observation of the desorption peak corresponding to the second layer (under different experimental conditions, not shown) allowed us to calibrate the Xe coverage. The thermal desorption (TD) spectrum for the saturated surface exhibits a well-resolved two-peak structure, with a peak at 82 K (denoted II in Fig. 5) and another at 92 K (denoted I in Fig. 5). For low Xe coverages only peak I is observed. The maximum of this peak is at 100 K, shifting to lower temperatures as the exposure of Xe increases. Beyond 2 L (where 1 L$=10^{-6}$ Torr s) the position is stabilized at 92 K. From 5 L on a broadening on the low-temperature side is observed, which is indicative of the population of a new kind of adsorption site. This broadening evolves into a well-developed maximum at 82 K. A comparison of the peak heights suggests that the number of adsorption sites corresponding to the desorption maxima is nearly equal. This is reasonable within the dimer model for the Si(100)2×1 surface, as two types of sites are expected for Xe adsorption (see also Sec. III B 3): pedestal-bridge (II in Fig. 1) and cave-valley (I in Fig. 1) sites, each corresponding to a different coordina-

tion of Xe atoms with the substrate Si atoms. The desorption energies are 175 and 202 meV/atom, respectively.[55]

2. *Ultraviolet photoemission spectroscopy of adsorbed xenon*

We have used photoemission of adsorbed xenon (PAX) to reveal the lateral inhomogeneities of the surface potential. For a detailed description of the technique, we refer the reader to Refs. 58 and 59. Very briefly, the binding energy (BE) of the 5*p* levels of adsorbed Xe atoms is pinned to the vacuum level, independently of the substrate nature. This property converts the binding energy of the Xe levels with respect to the Fermi energy of the substrate in a tool able to probe the local work function at the adsorption site.

Figure 6 shows a set of ultraviolet photoemission (UP) spectra of the 5*p* level of Xe atoms adsorbed on the Si(100)2×1 surface, corresponding to 0.5 and 11 L Xe exposure. The 5*p* peaks apparently contain no structure or asymmetry. The coverage dependence of the full width at half maximum (FWHM) of both $5p_{1/2}$ and $5p_{3/2}$ peaks appears in the left panel of Fig. 6, where the difference of the FWHM of both peaks (Δ FWHM) is also represented versus the Xe exposure. Additional broadening of the $5p_{3/2}$ peak takes place already at a Xe coverage corresponding to 1 L exposure. On the other hand, the 5*p* peaks have been fitted by a set of Lorentzians following standard procedures (an example appears in the right panel of Fig. 6). Up to 3 L xenon exposure only one set of Lorentzians (one for the $5p_{1/2}$ peak and two for the $5p_{3/2}$ peak as is well known) is needed. The best fit was obtained assuming a splitting for the $5p_{3/2}$ level of 0.11 eV and a value of 1.30 eV for the energy difference between the $5p_{1/2}$ and $5p_{3/2}$ peaks. The experimental spectra beyond the exposure of 3 L have to be deconvoluted by using two sets of Lorentzians, which is in agreement with the occurrence of the second thermal desorption maximum in the TD spectra and with the increase of the FWHM of the $5p_{1/2}$ peak. This second state appears in the Xe-UP spectrum at a BE higher by 0.2 eV with respect to the first state. The area ratio of both states for saturation is 60% to 40%, respectively, which is in full agreement with the relative abundance of the two kinds of adsorption sites obtained by simulation of the experimental TD spectra.

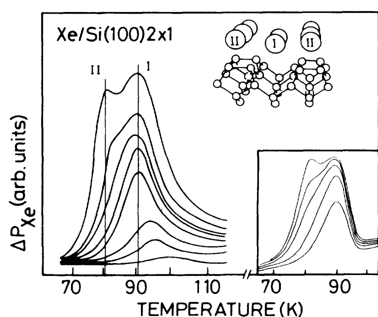

FIG. 5. Thermal desorption spectra for Xe adsorbed on a clean Si(100)2×1 surface. The traces correspond to increasing Xe exposures of 0.1, 0.5, 1.0, 2.0, 3.0, 4.0, 5.0, and 11 L from bottom to top. The Xe desorption peaks I and II are assigned to the Xe adsorption sites displayed in the perspective view of the surface and denoted as in Fig. 1 (see also text). Inset: numerical simulation of the experimental traces. The traces correspond (from bottom to top) to increasing initial Xe coverages of 0.30, 0.50, 0.70, 0.85, and 1.0 ML.

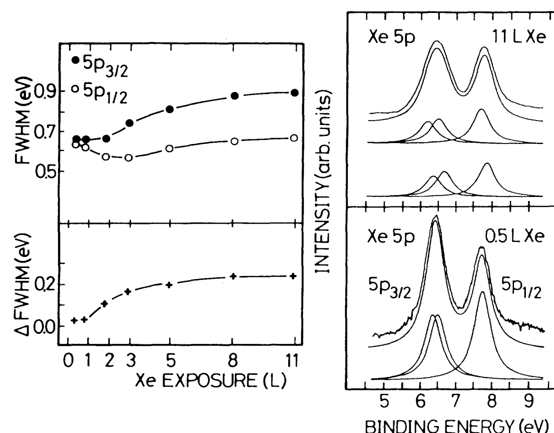

FIG. 6. Right panel: Xe 5*p* ultraviolet photoemission spectra for 0.5 and 11 L Xe exposure. Experimental curves and optimized fittings are shown. For 0.5 L only one component is needed for the $5p_{1/2}$ peak (at higher binding energy), while two components are needed for 11 L. Left panel: FWHM for the $5p_{1/2}$ and $5p_{3/2}$ Xe peaks vs Xe exposure, and incremental FWHM (Δ FWHM) between both peaks vs Xe exposure. Note the changes starting at 1–2 L exposure.

3. *Discussion*

The relatively simple structural model for the Si(100)2×1 surface enables one to establish a correlation between the two desorption maxima and possible xenon adsorption sites on the surface, a task much more complicated in the case of other Si surfaces.[60] Assuming that the Xe adsorption energy increases with the coordination number of the adsorption site, then the TD peak which develops first (92 K) should correspond to adsorption in the cave sites. The second Xe peak at 82 K corresponds then to adsorption on top of the rows of dimers (pedestal sites). This intuitive approach is fully supported by model calculations of the bonding energy of a xenon atom at each of the four adsorption sites (pedestal, bridge, cave, and valley, see Fig. 1), assuming a simple pairwise summation of Lennard-Jones (6-12) potentials between the Xe atoms and the substrate atoms.[61–63] Thus we conclude that the peak at 92 K corresponds to xenon atoms adsorbed on the cave sites. Once these sites are completely occupied by xenon atoms, only the sites over the dimer rows remain free for further adsorption. In consequence, we attribute the peak at 82 K to adsorption on the pedestal sites (see Fig. 1). Note that due to a misprint error, the assignment of the two Xe desorption peaks was wrongly made in Ref. 35, where preliminary results of

our work were presented. The relative intensities of both peaks are in reasonable agreement with the expected values for this surface.[64]

IV. THE K/Si(100)2×1 INTERFACE: RESULTS AND DISCUSSION

In order to ascertain the geometric and electronic properties of the K/Si(100)2×1 interface we will establish a careful coverage calibration, cross-checked by different techniques (AES, xenon TDS, PAX, potassium TDS). We have studied the temperature dependence of the growth of K multilayers. The possibility of lowering the temperature down to 40 K allowed us to study the Schottky-barrier formation by means of SPV saturation. We have also obtained the work-function change versus K coverage at RT and 50 K, and studied the local versus nonlocal nature of the work-function change by means of PAX.

A. Coverage calibration

Some contradictions exist in the literature about important properties of the interface, as saturation coverage, work-function change upon deposition, etc. Tochihara[8] reported a maximum change in the work function with respect to the clean surface of $\Delta\phi=2.1$ eV. Enta *et al.*[14,23] obtained saturation at a ratio of $I(K_{252})/ISi_{92})=0.47$ and $\Delta\phi=3.3$ eV. Both authors observed no minimum in the work-function curve. Oellig and Miranda[21] observed that up to ~2 ML of K grow at RT, and a minimum in the work-function curve at $\Delta\phi=3.0$ eV. In the case of Na/Si(100)2×1, Glander and Webb obtained[65] a saturation coverage of 0.68 ML.

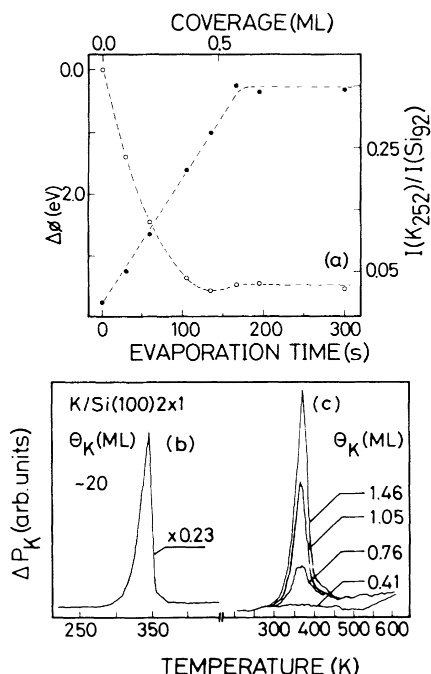

FIG. 7. (a) Work-function change (left-hand scale, open circles) and relative AES intensity ratio $I(K_{252})/I(Si_{92})$ (right-hand side scale, full circles), upon adsorption of K on Si(100)2×1 at 325 K, vs evaporation time. The flattening of the curves from ~170 s of evaporation indicates a coverage saturation of $\Theta_K=0.60$ ML. Lower panel: potassium thermal desorption. The experimental thermal desorption traces for potassium are shown. Curve (b): ~20 ML, heating rate 0.4 K/s, adsorption temperature, 55 K; curves (c): increasingly higher coverages up to 1.46 ML, heating rate 1 K/s, adsorption temperature, 273 K.

In this paper, potassium was deposited at 55 K. The surface was then annealed to 273 K during one minute. We have found that if either the annealing temperature (for one minute anneal) or the potassium deposition temperature are larger than 325 K, no more than 0.6 ML of K can be adsorbed. As shown in Fig. 7(a), at 325 K the AES intensity ratio $I(K_{252})/I(Si_{92})$ increases linearly with deposition time, but only up to a certain value, after which it remained constant at a value of 0.35. At this temperature a work-function decrease of 3.3 eV is measured (compare to Fig. 9, Sec. IV C), but only a shallow minimum is observed at $I(K_{252})/I(Si_{92})=0.28$, a behavior very similar to that found by some authors.[14,23]

We assign the minimum in the work function observed at $I(K_{252})/I(Si_{92})=0.28$ (see also Sec. IV C) to a K coverage of 0.5 ML on the basis of xenon desorption experiments (see Sec. IV E for details on the experiments and the adsorption model assumed). This assignment agrees with the association made by many authors between the minimum of the work function and a coverage of 0.5 ML (Ref. 29, and references therein). For $\Theta_K \geq 0.5$ ML, the coverage was measured also using the AES ratio, calibrated considering the value corresponding to 1 ML as determined by Xe TDS.

Our data of potassium desorption indicate that multilayer adsorption at 273 K is possible. Figure 7(b) shows the desorption of a thick (20 ML) potassium film deposited at 55 K. The peak follows zeroth-order desorption kinetics, which is typical for the sublimation process. This thermal desorption spectrum provided us with a kind of internal temperature scale. Thermal desorption data for smaller amounts of potassium adsorbed at 273 K are presented in Fig. 7(c). When the adsorption temperature was increased to only 325 K no more desorption peak in the range presented in Fig. 7(c) could be detected.

B. Adsorption energy of potassium

We have evaluated the adsorption energy of potassium by performing stepwise thermal desorption (STD). The K-covered substrate was annealed to increasingly higher temperatures during 1 s, and the remaining K coverage was evaluated by means of AES. We followed the method proposed by Rawlings *et al.*[66] in order to evaluate the adsorption energy (E_{ad}) as a function of coverage, assuming a preexponential factor of $\nu=10^{13}$ s^{-1}. By this method an approximate value of E_{ad} (averaged over a finite $\Delta\Theta_K$ range) is obtained. Figure 8(a) presents the evolution of the coverage versus annealing temperature, while Fig. 8(b) shows the dependence of E_{ad} versus coverage, both in the range between 0.1 and 0.7 ML. The results agree reasonably well with the values obtained by Tanaka *et al.*[67]

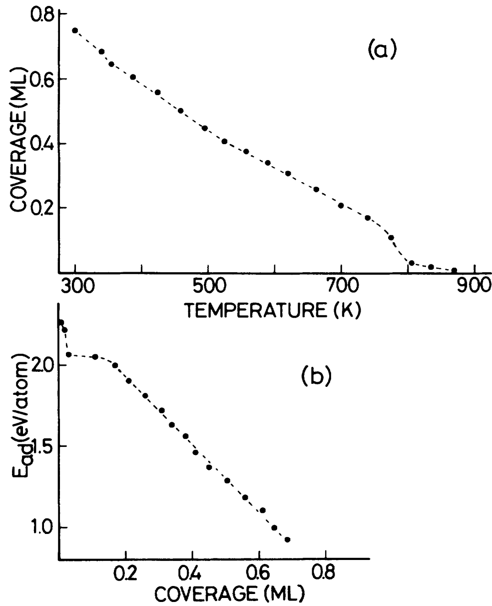

FIG. 8. Stepwise thermal desorption of K. The K-covered surface was annealed 1 s to increasingly higher temperatures. The dashed lines are a guide to the view. In (a) the amount of K left on the surface is represented vs the annealing temperature. (b) displays the K adsorption energy vs K coverage (see text for details).

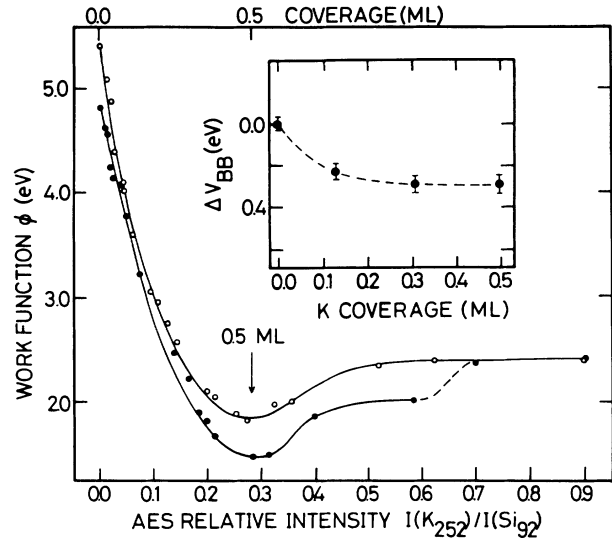

FIG. 9. Surface work function vs K coverage (upper scale) and vs the $I(K_{252})/I(Si_{92})$ Auger peak ratio (lower scale). Black dots: surface at 55 K; white circles: sample at room temperature. Note that both curves coincide for $I(K_{252})/I(Si_{92})$ larger than 0.6–0.7. Inset: band-bending change vs K coverage obtained from the temperature dependence of the K-induced work-function change.

C. Work-function measurements

The variation of the work function of the Si(100)2×1 surface due to the potassium adsorption was monitored at 55 and 273 K, and is presented in Fig. 9. Note that due to the linearity of the ratio $I(K_{252})/I(Si_{92})$ versus Θ_K (for $\Theta_K \leq 0.5$ ML), the upper scale in Fig. 9 is also linear for this coverage range. From Fig. 9 it is clear (see also Ref. 35) that both work-function curves decrease rapidly in the low coverage regime. Further deposition of potassium reduces the slope of the $\Delta\phi(\Theta)$ curve, indicating depolarization effects characteristic of the alkali-metal adsorption.[21] The minimum corresponds to an $I(K_{252})/I(Si_{92})$ ratio of 0.28.

The room-temperature work-function change exhibits a larger decrease than the low-temperature one. This is due to the fact that at any coverage the room-temperature curve includes the change of the surface dipole and band bending, whereas the low-temperature curve includes the change in the surface dipole moment only.

The coverage dependence of the band bending induced by potassium adsorption was measured the first time by using the SPV effect. The experimental points are displayed versus K coverage in the inset of Fig. 9. The decrease of band bending saturates around $\Theta_K=0.25$ ML, at a value of 0.30 eV, thus indicating that the K-Si interface potentials are completely defined after deposition of 0.25–0.30 ML of K, in good agreement with theoretical calculations.[29]

Finally, note that the points corresponding to the higher K coverages in Fig. 9 in fact coincide (the absolute value of the work function ϕ is identical at 273 and 55 K). At these metal coverages the mechanisms responsible for the SPV are not longer active. We conclude that for a K coverage between 0.8 and 1.0 ML [which corresponds to an $I(K_{252})/I(Si_{92})$ ratio of 0.6 and 0.7, respectively, dashed line if Fig. 9], the electron-hole pair recombination rate was increased so that SPV could not be saturated any longer. This behavior indicates that the surface is in fact metallic at this coverage.

D. Valence-band spectroscopy of K/Si(100)2×1 surface

The angle-integrated UP spectrum of the K/Si(100)2×1 interface shows no prominent features for coverages below 0.5 ML. The region around the Fermi energy appears in Fig. 4 for different K coverages, and also for a thick K film (see the inset in Fig. 4). The emission at the Fermi energy is completely defined at a coverage of 1 ML, and starts to grow from 0.5 ML, being clearly visible at 0.8 ML. The observation of the Fermi level in the UP spectrum at 1 ML is a direct proof of the metallic character of the interface at this coverage. This evidence supports that the K atoms donate only a fraction of the 4s electron to the silicon atoms, in good agreement with recent MDS experiments.[25] The inset in Fig. 4 shows the spectrum obtained for a thick (~20 ML) K film. The density of states has the typical triangular shape observed for alkali metals.[68] The sharp peak at a BE of 3.8 eV is an Auger $M_{2,3}VV$ transition of 17.4 eV kinetic energy, which is detected at this apparent binding energy with 21.2-eV photons.

E. Thermal desorption of Xe from K/Si(100)2×1

Potassium was deposited on Si(100)2×1 at 55 K, and the covered surface was annealed one minute at 273 K. The surface was then cooled down to 50 K. The amount of K present at the surface was not affected by the annealing process, as judged by AES. The interface so prepared was then exposed to 10^{-8} Torr of Xe during a time long enough to saturate the surface. Extensive studies showed that xenon does not adsorb on top of potassium under these conditions, and only occupies the free sties of the Si surface. In fact, the adsorption energy of Xe atoms on top of K atoms is expected to be much lower than on Si atoms.[69,70] Figure 10 shows a series of Xe-TD traces corresponding to increasingly higher potassium coverages. It is evident from the traces that the increase of the potassium coverage is accompanied by the suppression of the high-temperature component of the xenon traces (peak I, at 92 K). A numerical simulation of the spectra has shown that the amount of xenon adsorbed at saturation decreases in a nearly linear proportion with the amount of potassium adsorbed. Moreover, a comparison of the areas indicates that the area under the spectrum *d* is nearly half of the area under the spectrum *a*. We can conclude that potassium deposition does not alter the properties of the free sites at the silicon surface (from the point of view of the xenon adsorption energy).

In addition, the elimination of the peak at 92 K means that potassium atoms block the surface sites responsible for this signal. Since these sites correspond to cave-valley sites (see Sec. III B 3), we conclude that potassium atoms (in these annealed overlayers) are preferentially adsorbed on the cave-valley sites of the 2×1 reconstruction.

It is to be noted that the AES peak height ratio K/Si for the spectrum *d* corresponds to 0.55 ML according to our coverage calibration, i.e., we have found that the minimum in the work function corresponds to the amount of K which quenches the Xe-TDS peak I of Fig. 10. This, in turn, is close to the coverage that can be deposited at 325 K [Fig. 7(c)]. It is reasonable to assign this coverage to 0.5 ML, since the Xe-TDS peak II is not quenched at all. In this way an internally consistent determination of the absolute coverage can be obtained.

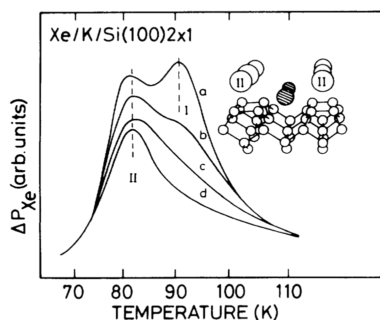

FIG. 10. Thermal desorption spectra for saturation of Xe on a clean Si(100) surface (curve *a*) and covered with 0.18 (curve *b*), 0.38 (curve *c*), and 0.55 (curve *d*) ML of potassium, respectively. In all cases the K adlayer was annealed to 273 K, then cooled to 55 K and exposed to 30 L Xe. The perspective view of the surface shows schematically K adatoms (dashed) occupying the cave sites and Xe adatoms adsorbed at the pedestal sites (II).

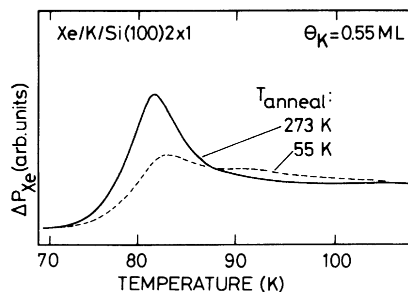

FIG. 11. Temperature dependence of the K-atom distribution between cave and pedestal sites. The K adlayer was deposited at 55 K, and the surface then exposed to 30 L of Xe. When the adlayer is annealed to 273 K prior to Xe exposure (continuous line), the K adatoms occupy only the cave sites. If the adlayer is not annealed, the K adatoms occupy both pedestal and cave sites (dashed line).

We obtained Xe-TD traces for nonannealed adlayers as well. Figure 11 shows two curves for an amount of 0.55 ML of K. In the case of the annealed adlayer K atoms have fully populated the cave sites. In the case of nonannealed adlayers, the blocking by K atoms of pedestal sites is more efficient, and in addition a small number of cave sites are left free. This indicates that the ordering of the nonannealed K adlayer is much worse, and a broad distribution of Xe adsorption sites exists. The total Xe uptake is somewhat reduced in this case, because the less-ordered distribution of the K atoms blocks the surface more effectively for Xe adsorption.

F. Potassium-induced local work-function change

The most conspicuous experimental feature about alkali-metal adsorption on semiconducting surfaces is the strong reduction induced in the work function of the surface.[3] The methods usually employed to measure the work-function changes (Kelvin probe, photoelectron spectroscopy) average over the surface of the sample. It is highly desirable to detect the work-function changes induced by alkali-metal deposition with lateral resolution, in order to assess the extent of the modification in the electrostatic potential. In this way it could be determined whether those changes are more pronounced in the vicinity of the alkali-metal adatoms and how they involve the clean (i.e., not covered by alkali-metal adatoms) patches of the semiconducting silicon surface.

Mainly two experimental techniques, STM and PAX, are currently able to resolve lateral inhomogeneities in the surface electrostatic potential. We set out to experimentally determine by means of PAX the eventual lateral inhomogeneities in the surface electrostatic potential brought about by alkali-metal adsorption on semiconducting surfaces.

It should be expected that the dramatic work-function decrease of the Si(100)2×1 surface due to potassium adsorption should also induce a significant shift of the xenon 5*p* levels to higher BE. To demonstrate the influence

of the potassium overlayer on the Xe 5*p* levels, selected UPS spectra of the Xe 5*p* lines, corresponding to potassium coverages ranging from 0 to 0.55 ML, and exposed to 1 L of xenon, have been plotted in Fig. 12. The xenon exposure was chosen such that the Xe atoms are adsorbed always (at least for small K coverages) only on the cave sites. As expected, the 5*p* peaks shift to higher binding energies with increasing K coverage. The total shift is 2.0 eV for $\Theta_K=0.55$ ML.[71] In addition, already for very small potassium coverage the Xe 5*p* spectra exhibit a peak asymmetry. For $\Theta_K=0.04$ ML, a shoulder on the high-binding-energy side of the $5p_{1/2}$ peak is clearly seen. With increasing potassium coverage the shoulder intensity increases, and, at $\Theta_K=0.12$ ML, develops into a new peak. This asymmetry of the 5*p* peaks arises from the superposition of two spectra of Xe adsorbed on two different adsorption sites. These two states are separated by 0.5 eV and can be interpreted as corresponding to Xe atoms adsorbed next to K atoms [higher-binding-energy state, in the following we shall refer to this state as Xe(K/Si)] and further away from K atoms [lower-binding-energy state, in the following we shall refer to this state as Xe(Si)]. The separation of 0.5 eV represents an enhanced local decrease in the surface potential next to K atoms (at the Xe probing distance) with respect to the overall shift, which is due to a K-induced long-range decrease of the surface potential. Thus these data directly illustrate the twofold effect of K adsorption on Si: long and short range. Note that the change in the 5*p* peak line shape with potassium coverage is consistent with the model, as the intensity of the Xe(K/Si) state increases for higher K coverages. The spectrum of the clean Si(100)2×1 surface can be fitted with a single set of three Lorentzians [one for the $5p_{1/2}$ level and two for the $5p_{3/2}$ (see Sec. III B)] for this xenon exposure (1 L). The BE of the $5p_{1/2}$ peak is 7.80 eV below the Fermi energy. This peak corresponds to Xe atoms sitting in cave-valley positions on the clean Si patches. When potassium adatoms are present on the surface, two kinds of Xe states are observed in the experimental data. They differ because of the different electrostatic potential they feel. Computer decomposition of all the experimental spectra is possible with only two sets of Lorentzians. An example of the results of the fit is also shown in Fig. 13. The set of Lorentzians at lower BE (labeled *A* in Fig. 13) represents the Xe atoms adsorbed on the clean patches of the surface, while the Lorentzian set at higher BE (labeled *B* in Fig. 13) corresponds to the Xe atoms adsorbed in the vicinity of the K adatoms. Upon increasing the K coverage, further Xe atoms come into contact with K adatoms and are affected by their influence on the electrostatic potential.[71]

At a potassium coverage of 0.04 ML the Xe(Si)-$5p_{1/2}$ peak is shifted by around 0.23 eV with respect to the position found for the clean surface. This shift is in a certain way a measure of the long-range perturbation of the silicon surface due to potassium adatoms. It is interesting to compare these values with corresponding findings for K adsorption on a metal. On the K/Ru(100) surface, Markert and Wandelt[72] reported that the short-range effect is 0.57 eV [energy difference between the 5*p* levels corresponding to Xe(K/Ru) sites and to Xe(Ru) for the clean surface], while the long-range effect [energy difference between the Xe(Ru) state for the clean surface and the same state for the K-covered surface] is only 0.08 eV. This indicates that the local potential perturbation due to the presence of K adatoms is very similar on the Ru and Si surfaces. On the other hand, the smaller long-range effect detected on Ru can be related to the smaller screening length of Ru as compared to Si.

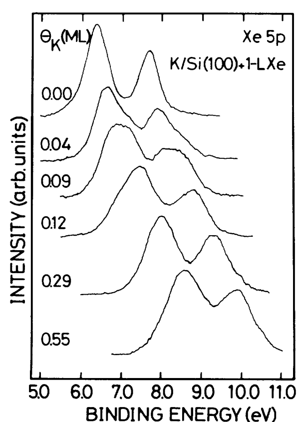

FIG. 12. Xe 5*p* ultraviolet photoemission spectra taken at different K coverages. Note the K-induced shoulder appearing already at 0.04 ML, which evolves into the main peak at higher coverages. Note also the overall shift of the spectra to higher binding energy.

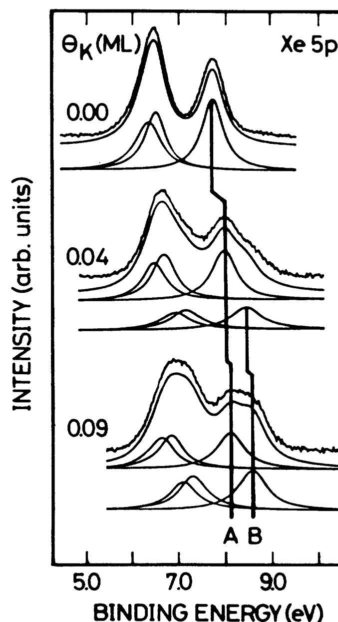

FIG. 13. Selected Xe 5*p* ultraviolet photoemission spectra showing the deconvolution in two components *A* and *B*. The state *B* corresponds to Xe atoms adsorbed on silicon at sites close to K adatoms; the state *A* corresponds to Xe atoms adsorbed on silicon at sites farther away from K atoms.

V. DISCUSSION

The experimental results presented in this paper, together with the previously existing work, provide us with a consistent picture of the K/Si(100)2×1 interface from the experimental point of view.

Some considerations should be made on coverage calibration. Inadequate coverage calibrations have given rise to many of the problems found in correctly interpreting the experimental results on this system. Most workers have attributed a coverage of 0.5 ML to the minimum of the work-function curve, which is a correct assignment according to our results. Work-function measurements at RT indicate that the reduction of the work function is 3.3 eV. Only Tochihara in his pioneering work on this system[8] reported a value of 2.1 eV, which has not been reproduced by other authors. Probably the actual coverage was too low or the sample was inadequate due to imperfections or impurities.

Enta *et al.*[14,23] concluded that their RT saturation coverage was 1.0 ML, obtained for $\Delta\phi=3.3$ eV. Assuming our value of 0.6 ML for this coverage, their results are in full agreement with ours, as they observe a Fermi-level onset for coverages slightly above the saturation one.[23] Their assignment of 1 ML to the saturation coverage agrees with the theoretical prediction of a semiconducting character for surface at this coverage. For models assuming total charge transfer at all coverages,[10,13] the surface would be actually semiconducting at 1 ML, but these models are not supported by recent MDS experiments,[25] showing that the charge transfer is small even at very low coverages.

The second point of interest is the strength of the K—Si bond. It should be noted that the growth of multilayers of K at 273 K is certainly possible, but the stability of the multilayers decreases quickly as temperature is raised above ~300 K. Saturation of the amount of K present on the surface at temperatures close to RT, as found by many workers,[8,14,23,32,33] can be explained as an effect due to a slightly too high sample temperature. It is difficult to establish the exact value for the adsorption energy on the basis of desorption data, as has been shown previously by several authors.[73] However, an estimate of the adsorption energy can be directly obtained from the temperature of desorption (Redhead method[56]). As the desorption for coverages over 0.5 ML takes place at temperatures close to those observed for a thick K layer, also a similar E_{ad} is obtained (~ 1.0 eV/atom for $\nu=10^{13}$ s^{-1}). For $\Theta \leq 0.5$ ML values of $\sim 1.5-2$ eV/atom have been obtained by STD.

Metallization is accompanied by definition with the appearance of a band crossing the Fermi energy. For RT saturated surfaces, no emission at the Fermi energy has been detected.[14,23] When the surface is metallized, an emission at the Fermi energy should appear. In this sense, the surface is not metallic at 0.6 ML. The onset at the Fermi level, however, can be difficult to detect by photoemission measurements if a substantial density of states at the Fermi energy is not present. In fact, due to the small UPS cross section of *s*-like states, the measured density of states at the Fermi energy is very low even for a bulklike alkali-metal film (see Fig. 4). By using different techniques we have found various upper limits to the actual coverage at which metallization takes place. Our results indicate that at least at 0.8 ML the surface is metallic, by the appearance of the Fermi-level cutoff. The disappearance of the SPV at ~ 0.8 ML also indicates that at this coverage a substantial density of states exists at the Fermi level. Considering the behavior of adsorbed potassium against O_2 exposure,[15,42,74] metallization could already occur at 0.5 ML, because for $\Theta_K \geq 0.5$ ML the surface displays during O_2 adsorption similar features in UPS and work-function changes to those in thick K layers. Other evidence suggesting such a metallization at around 0.5 ML has been obtained by observing the energy losses of the K 2*p* peak,[29] which could be associated to surface plasmons, although an interband transition can also originate the observed effect. Whether the possible metallization at $\Theta_K=0.5$ ML will correspond to the K overlayer or to the Si surface is a problem difficult to solve with the available data for this particular coverage. However, the observed metallization remains for $\Theta_K=1.0$ ML. At this coverage intense Fermi-level emission is observed (see Fig. 4), and so the models predicting a semiconducting surface at this coverage should be discarded.

Concerning the K adsorption site, our results indicate that the cave-valley sites are first occupied, in agreement with some theoretical calculations,[12,11] and other experimental evidence.[39,40] The adsorption at the on-top site for very low coverage[37] could be possible, but this site does not seem to be favored for higher coverages.[41] Our observations are in agreement with XPD,[32,33] AED,[34] and LEED (Ref. 75) results. Since the actual coverage at temperatures around 300 K can be over 0.5 ML, the amount of K atoms at the surface can exceed the number of cave sites. This would naturally explain the formation of a (not-completed) double layer as pointed out in Refs. 32 and 33, where the measurements were taken for the saturation coverage at RT. If the adlayers are not well ordered, the percentage of adatoms sitting at pedestal sites can be even higher (see Sec. IV E and Fig. 11).

VI. CONCLUSIONS

In summary, the picture of the system K/Si(100)2×1 obtained from the experimentally observable properties can be described as follows. The interaction between K and Si gives rise to an intense work-function change, which for very low coverages takes place basically around the K sites. The work function diminishes and reaches a minimum at $\Theta_K=0.5$ ML with $\Delta\phi=3.3$ eV at RT. Further growth of K is possible at 273 K, and the adsorption energy of K adatoms on Si(100) ranges between 1.5 and 2 eV depending on the coverage. The Schottky-barrier formation is accompanied by a band-bending change at the surface of 0.3 eV, and the barrier is formed at ~ 0.25 ML ($\sim 50\%$ of the first half of a monolayer). Detectable photoemission from the Fermi level appears between 0.5 and 0.8 ML. The surface remains metallic after deposition of 0.5 ML up to multilayers.

ACKNOWLEDGMENTS

We thank Dr. R. Ramírez for fruitful discussions. This work was supported by the Deutsche Forschungsgemeinschaft through Sonderforschungsbereich 6, which granted the research stays of E.G.M. and R.M. G.R.C. acknowledges his support by the Alexander-von-Humboldt-Stiftung and P.P. is grateful for a grant from the Internationales Büro der KFA Jülich (BMFT).

*Permanent address: Departamento de Fisica de Materia Condensada C-III, Universidad Autonoma de Madrid, 28049-Madrid, Spain.

†Permanent address: Institute of Physics of the University, Zagreb, Croatia.

[1]For a number of excellent reviews see, for example, *Physics and Chemistry of Alkali Metal Adsorption,* edited by H. P. Bonzel, A. M. Bradshaw, and G. Ertl (Elsevier, Amsterdam, 1989).

[2]For a recent, comprehensive review, see for example, *Metallization and Metal-Semiconductor Interfaces,* edited by I. P. Batra (Plenum, New York, 1988).

[3]J. D. Levine, Surf. Sci. **34**, 90 (1973).

[4]W. E. Spicer, Appl. Phys. **12**, 115 (1977).

[5]A. Franciosi, P. Soukiassian, P. Philip, S. Chang, A. Wall, A. Raisanen, and J. Troullier, Phys. Rev. B **35**, 910 (1987).

[6]M. C. Asensio, E. G. Michel, E. M. Oellig, and R. Miranda, Appl. Phys. Lett. **51**, 1714 (1987).

[7]L. J. Brillson, Surf. Sci. Rep. **2**, 123 (1982).

[8]H. Tochihara, Surf. Sci. **126**, 523 (1983).

[9]D. Haneman, Rep. Prog. Phys. **50**, 438 (1987).

[10]S. Ciraci and I. P. Batra, Phys. Rev. B **37**, 2995 (1988).

[11]Y. Ling, A. J. Freeman, and B. Delley, Phys. Rev. B **39**, 10 144 (1989).

[12]R. Ramírez, Phys. Rev. B **40**, 3962 (1989).

[13]S. Ciraci and I. P. Batra, Phys. Rev. Lett. **56**, 877 (1986).

[14]Y. Enta, T. Kinoshita, S. Suzuki, and S. Kono, Phys. Rev. B **36**, 9801 (1987).

[15]G. R. Castro, P. Pervan, E. G. Michel, R. Miranda, and K. Wandelt, Vacuum **41**, 564 (1990).

[16]T. Kendelewicz, P. Soukiassian, R. S. List, J. C. Woicik, P. P. Pianetta, I. Lindau, and W. E. Spicer, Phys. Rev. B **37**, 7115 (1988).

[17]I. P. Batra, Phys. Rev. B **39**, 3929 (1989).

[18]T. Aruga, H. Tochihara, and Y. Murata, Phys. Rev. Lett. **33**, 372 (1984).

[19]H. Ishida, N. Shima, and M. Tsukada, Phys. Rev. B **32**, 6246 (1985).

[20]H. Ishida, N. Shima, and M. Tsukada, Surf. Sci. **158**, 438 (1985).

[21]E. M. Oellig and R. Miranda, Surf. Sci. **177**, L947 (1986).

[22]J. E. Ortega, E. M. Oellig, J. Ferron, and R. Miranda, Phys. Rev. B **36**, 6213 (1987).

[23]Y. Enta, T. Kinoshita, S. Suzuki, and S. Kono, Phys. Rev. B **39**, 1125 (1989).

[24]Y. Enta, S. Suzuki, S. Kono, and T. Sakamoto, Phys. Rev. B **39**, 5524 (1989).

[25]S. Nishigaki, S. Matsuda, T. Sasuki, N. Kawanishi, Y. Ikeda, and H. Takeda, Surf. Sci. **231**, 271 (1990).

[26]P. S. Bagus and I. P. Batra, Surf. Sci. **206**, L895 (1988).

[27]I. P. Batra and P. S. Bagus, J. Vac. Sci. Technol. A **6**, 600 (1988).

[28]R. V. Kasowski and M. H. Tsai, Phys. Rev. Lett. **60**, 546 (1988).

[29]E. M. Oellig, E. G. Michel, M. C. Asensio, R. Miranda, J. C. Duran, A. Muñoz, and F. Flores, Europhys. Lett. **5**, 727 (1988).

[30]H. Ishida and K. Terakura, Phys. Rev. B **40**, 11 519 (1989).

[31]R. Holtom and P. M. Gundry, Surf. Sci. **63**, 263 (1977).

[32]T. Abukawa and S. Kono, Phys. Rev. B **37**, 9097 (1988).

[33]T. Abukawa and S. Kono, Surf. Sci. **214**, 141 (1989).

[34]M. C. Asensio, E. G. Michel, J. Alvarez, C. Ocal, R. Miranda, and S. Ferrer, Surf. Sci. **211/212**, 31 (1989).

[35]P. Pervan, E. G. Michel, G. R. Castro, R. Miranda, and K. Wandelt, J. Vac. Sci. Technol. A **7**, 1885 (1989).

[36]D. Badt, A. Brodde, St. Tosch, and H. Neddermeyer, J. Vac. Sci. Technol. A **8**, 251 (1990).

[37]Y. Hasegawa, I. Kamiya, T. Hashizume, T. Sakurai, H. Tochirara, M. Kubota, and Y. Murata, Phys. Rev. B **41**, 9688 (1990).

[38]This site corresponds to adsorption on top of the protruding Si atom of a buckled dimer.

[39]J. Binder, U. A. Ditzinger, M. Hanbücken, Ch. Lunau, K. Wieschermann, and H. Neddermeyer, Europhysics Conference Abstracts (ECOSS 11—European Conference on Surface Science) **14G**, 222 (1990); (private communication).

[40]V. Eteläniemi, E. G. Michel, and G. Materlik, Surf. Sci. **251/252**, 483 (1991).

[41]I. P. Batra, J. Vac. Sci. Technol. A **8**, 3425 (1990).

[42]G. R. Castro, P. Pervan, E. G. Michel, R. Miranda, and K. Wandelt, Vacuum **41**, 787 (1990).

[43]W. F. Egelhoff, Surf. Sci. Rep. **6**, 253 (1987).

[44]H. G. Gatos and J. Lagowski, J. Vac. Sci. Technol. **10**, 130 (1973), and references therein.

[45]J. Demuth, W. J. Thompson, N. J. DiNardo, and R. Imbihl, Phys. Rev. Lett. **56**, 1408 (1986).

[46]S. M. Sze, *Physics of Semiconductor Devices* (Wiley, New York, 1981).

[47]P. S. Kirev, *Semiconductor Physics* (Mir, Moscow, 1974).

[48]L. J. Brillson, J. Vac. Sci. Technol. **16**, 1137 (1979).

[49]R. J. Hamers, R. M. Tromp, and J. E. Demuth, Phys. Rev. B **34**, 5343 (1986).

[50]F. J. Himpsel and D. E. Eastman, J. Vac. Sci. Technol. **16**, 1297 (1979).

[51]A. L. Wachs, T. Miller, T. C. Hsieh, A. P. Shapiro, and T. C. Chang, Phys. Rev. B **32**, 814 (1984).

[52]F. J. Himpsel and T. Fauster, J. Vac. Sci. Technol. A **2**, 814 (1984).

[53]A. Goldmann, P. Koke, W. Mönch, G. Wolfgarten, and J. Pollmann, Surf. Sci. **169**, 438 (1986).

[54]W. Mönch, P. Koke, and S. Krueger, J. Vac. Sci. Technol. **19**, 313 (1981).

[55]The multipeak structure prevents a parameter-free analysis. Therefore we applied the Redhead method (Ref. 56). Assuming $\nu = 10^{12}$ s^{-1} (preexponential factor) we get desorption energies of 192 and 212 meV/atom, respectively, for the peaks at 82 and 92 K. Using these values the experimental TD

traces have been numerically simulated (see the inset in Fig. 5). The best agreement with the experimental spectra (in line shape and coverage dependence) has been obtained assuming a ratio of 40% to 60% for the relative availability of adsorption sites corresponding to both TD peaks. In addition, since closer inspection of the TD spectra shows an equilibrium in the population of the two kinds of adsorption sites, the TD spectra have been simulated by calculating the equilibrium distribution of adsorbed Xe atoms assuming the Fermi distribution (Ref. 57). Although the peak position and line shapes were correctly reproduced, the full width at half maximum (FWHM) of the simulated spectra were too small compared to the experimental ones. Therefore a smaller preexponential factor was assumed ($\nu = 10^{11}$ s^{-1}). By use of the Redhead method we obtained desorption energies of 175 and 202 meV/atom, respectively. These new values reproduce quite well the peak positions and the width of the spectra (see Fig. 5).

[56]P. A. Redhead, Vacuum **12**, 203 (1962).

[57]J. W. Bartha, Ph.D. thesis, University of Hannover (F.R.G.), 1983.

[58]K. Wandelt, in *Thin Metal Films and Gas Chemisorption*, edited by P. Wissmann (Elsevier, Amsterdam, 1987).

[59]K. Wandelt, in *Chemistry and Physics of Solid Surfaces VIII*, edited by R. Vanselow and R. Howe, Springer Series in Surface Science Vol. 22 (Springer, Berlin, 1990), p. 289.

[60]J. E. Demuth and A. J. Schell-Sorokin, J. Vac. Sci. Technol. A **2**, 808 (1984).

[61]E. Conrad and M. E. Webb, Surf. Sci. **129**, 37 (1983).

[62]G. Ehrlich and F. G. Hudda, J. Chem. Phys. **30**, 493 (1959).

[63]R. Ramírez (private communication).

[64]The experimental intensity ratio of both sites (40% to 60%) is not in full agreement with the expected values for the ideal dimer model (50% to 50%). This indicates that the number of high-coordination adsorption sites is larger than the number of cave-valley sites. In fact the presence of a certain amount of defect sites at the 2×1 surface prepared by sputtering is well known. Since the coordination number at the defect sites is close to the coordination at the cave sites, it is obviously why the thermal desorption intensity does not exhibit the 50% to 50% ratio. In addition the TD peak at temperatures higher than 92 K suggests the existence of a certain number of adsorption sites whose coordination is even higher than the coordination of the cave sites. The variation of the FWHM of the $5p_{1/2}$ peak with xenon exposure also supports the picture of xenon adsorption at defect sites at low xenon coverage. The decrease of the FWHM of the peak up to xenon exposure of 2 L suggests that xenon atoms are initially dispersed over the structurally different adsorption sites. For higher coverages the xenon atoms occupy structurally equivalent sites (cave sites as we concluded). The increase of the FWHM beyond 3 L exposure is in accordance with the population of an additional type of adsorption site (the pedestal sites). The variation of the incremental FWHM, correlated to the $5p_{3/2}$ splitting, indicates that below 1 L this splitting increases, and proceeds up to saturation coverage. This increase is due to Xe-Xe lateral interactions, i.e., the overlap of the $5p$ orbitals (Ref. 59). The increase in splitting clearly coincides with the population of the pedestal sites. The energy position of the second state (0.2 eV higher binding energy) corresponds to sites with lower coordination (Ref. 58) which fits quite well within our model.

[65]G. S. Glander and M. B. Webb, Surf. Sci. **222**, 64 (1989).

[66]K. J. Rawlings, S. D. Foulias, G. G. Price, and B. J. Hopkins, Surf. Sci. **118**, 47 (1982).

[67]S. Tanaka, N. Takagi, N. Minami, and M. Nishigima, Phys. Rev. B **42**, 1868 (1990).

[68]L. G. Petersson and S. E. Karlsson, Phys Scr. **16**, 425 (1977).

[69]E. Bertel, W. Jacob, and V. Dose, Appl. Phys. A **44**, 93 (1987).

[70]E. Bertel, W. Jacob, and V. Dose, Phys. Rev. B **36**, 2421 (1987), and references therein.

[71]All Xe-TDS and PAX spectra correspond to $\Theta_K \leq 0.6$ ML. As has already been pointed out, the adsorption energy of Xe on K is much lower than on Si. In fact, it was not possible to adsorb Xe dosewise on a K surface at 55-K substrate temperature. The application of a constant Xe pressure gave rise to the formation of three-dimensional Xe clusters as evidenced by the UPS spectra. This indicated that the Xe atoms do not wet the K surface, and also prevented the observation of adsorption of Xe *on top* of K atoms (for submonolayer K amounts) for fixed Xe doses. This site was observed only under constant Xe pressure (data not shown in this paper, see also Ref. 72 where a similar site is observed). The on-top site corresponds to the lowest local work function, and is not occupied by Xe atoms under our experimental conditions. Therefore the local work function is always larger than the average work function at the same coverage, because the Xe atoms do not probe the sites with lowest work function.

[72]K. Markert and K. Wandelt, Surf. Sci. **159**, 24 (1985).

[73]See, for example, D. A. King, Surf. Sci. **176**, L193 (1986) or E. Habenschaden and J. Küppers, *ibid.* **138**, L147 (1984), and references therein.

[74]G. R. Castro, P. Pervan, E. G. Michel, R. Miranda, and K. Wandelt (unpublished).

[75]T. Urano, Y. Uchida, S. Hongo, and T. Kanaji, Surf. Sci. **242**, 39 (1991).